An Organic Solar Cell Review: Polymer–Fullerene Based Bulk Heterojunction Devices & More

Han Liu

Abstract

As $> 10\%$ efficient organic solar cells (OSCs) have become growingly common, this literature review begins by outlining advantages of the emerging technology over its inorganic silicon-based competitors to provide motivations for studying the subject. With polymer-fullerene bulk heterojunction devices as the starting point, the overall efficiency of OSCs is decomposed into a product of the four fundamental underlying sub-processes: absorption, diffusion, dissociation and extraction. Then the four steps are examined individually from the perspectives of modelling and engineering with the goal of efficiency optimization in mind. To shorten the energy payback time and return factor, developments in green chemistry, performance stability as well as a few recyclable designs are also included in the life cycle analysis discussion. Finally, the review envisions a future forward from the bulk heterojunction and covers some non-binary or hybrid structures.

1.0 Introduction

Electricity generation by fossil fuels is becoming increasingly environmentally unpopular and economically infeasible. With fossil fuels responsible for 25% of the total harmful emission in the world annually, renewable energy businesses are gaining traction by the day [1]. Planet earth receives more energy from daily sunlight than the world's annual energy demand and solar cells offer an attractive alternative to tap into this limitless resource [2]. The global photovoltaic capacity grew from $6\,GW$ to $291\,GW$ from 2006 to 2016 and projects to exceed $540\,GW$ by 2021 [3]. Further, the manufacturing cost of solar modules decreased by nearly 74% from $\$1.85/W$ to $\$0.48/W$ in the same period [3]. As a direct consequence, renewables accounts for 72% of all the new energy sources installed in 2019 [1]. Photovoltaic cells, currently generating 9% of the world's total energy [4], alone have experienced exponential growth thanks to a decade of plunging solar prices. Building a solar energy generation plant is now cheaper than its fossil fuel counterpart and the days of subsidy incentivized profitability have officially come to an end [4].

Solar cell refers to devices capable of converting light into electrical energy. Photovoltaic effect was first discovered by Becquerel when he observed a photocurrent generated from illuminating silver halogen covered platinum

electrodes in 1839 [5]. Although the first observation of photoconductivity in an organic compound was reported by Pochettino in 1906, the first photovoltaic cell was a crystalline silicon based device developed at Bell laboratories in 1957 [5]. The first major breakthrough in organic solar cells (OSCs) came about when Tang discovered in 1986 that 1% efficiency could be achieved when an electron donor (D) layer was placed adjacent to its acceptor (A) counterpart in one cell [6]. In the following decades, the commercial success of OLED proved the viability of organic electronic components and sparked renewed interest in organic solar cell research. As a result, reports on OSCs with $>$ 10% power conversion efficiency have become increasingly common nowadays, thanks to the maturation of device designs, process optimization and interface engineering [7][8].

Solar cells can be classified into four generations. The first generation, currently most commercially available, comprised mostly of single- or multi-crystalline silicon and III-V wafer-based designs. The second generation heavily featured the usage of nanoscale thin films in response to the demand to reduce material usage and cost. The third generation explored the realm of OSCs. The fourth generation aims to bring forth a hybrid system combining the merits of all previous generations for optimal efficiency and cost [9]. The primary advantages of OSCs compared to their silicon predecessors are its general processability and applicability. Organic compounds enable inexpensive methods such as roll-to-roll manufacturing, inkjet printing and spin casting. In addition, unbounded from the rigid structure of silicon, OSCs may be installed everywhere, not just roof tops [6]. For example, Konarka is actively developing cells that may be incorporated into tents and clothes [2]. Commercially, Mitsubishi, Heliatek and Solarmer all offer flexible OSCs with power conversion efficiency (PCE) ranging from 8% to 13% [10][11][12].

Polymer fullerene based bulk heterojunction OSCs serve as the starting point of this review given its status as the upcoming emerging technology in photovoltaics. The review begins by examining the working principle of OSCs first by providing an overview of the photovoltaic process where fundamental concepts such as band theory and transition moment are mentioned briefly, along with references to more comprehensive reviews on the subjects. The review then dives deeper into details of the individual steps; they are absorption, diffusion, dissociation and extraction. The discussion is accompanied by outlining the challenges experienced in these processes and the novel solutions that have been designed to address them. Next, circuit models for OSCs are presented to provide readers the mathematical tools for quantifying the performance of OSCs. From there, the review shifts focus onto the recent developments in OSCs, featuring non-binary and hybrid bulk heterojunctions. Finally, a perspective on the life cycle of OSCs is presented

with an emphasis on improving energy payback time (EPT) and energy return factor (ERF).

2.0 The Working Principle of OSCs

As a broad overview, the photovoltaic process for OSCs consists of photon absorption, electron-hole pair generation, exciton diffusion, geminate dissociation, charge transport and collection [13]. In detail, a photon excites an electron in the highest occupied molecular orbital (HOMO) of D, promoting above the band gap, the hot carrier then relaxes to lowest unoccupied molecular orbital (LUMO) and causes phonon vibration. This process leaves behind a positive charge known as a "hole" at the same time, which can be conceptualized as the absence of an electron. The electron-hole pair is collectively referred to as an exciton, which may be considered an overall neutral particle that moves as a single entity. The Frenkel exciton has a smaller radius and its strong binding energy can be attributed to the low dielectric constants of organic materials, where an electron is more localized or confined to its parent molecule. The typical binding energy is on the $100\,meV$ scale, too large to be ionized thermally at room temperature [13]. The exciton generation and recombination processes are governed by the selection rule. Based on the selection rule, the transitional moment of said exciton generation is determined by the nucleus vibrational overlap, electron spin and spatial overlap based on the principle of symmetry and angular momentum conservation. The transition moment integral, which governs the transition from one quantum state to another, is responsible for phenomena such as Stoke's shift [14]. For more information on the selection rule, please refer to Chapter 7 of Atomic Physics by Paul Ewart [15]. Following the concentration gradient, an exciton diffuses towards the nearest D-A interface. If the exciton reaches the interface before recombination occurs and the D-A energy mismatch renders dissociation energetically favorable, then the electron and hole form a charge transfer state with the electron on the acceptor and the hole on the donor. Geminate pair dissociation remains an active area of research, which will be discussed in more details in the following sections [16]. An energy level diagram within the active layer is provided in Figure 1 with the aim to facilitate understanding of the description provided thus far. Under influence of the electric field, resulting from the asymmetrical electrode work functions, the hole drifts through the donor domain toward the anode and the electron drifts through the acceptor domain toward the cathode. This migration to the electrodes separately in opposite directions is the eventual step of charge collection. It is worth noting that the diffusion lengths of excitons are typically in the nanometer range, much smaller than the penetration depth of photons. As a result, most excitons are lost through recombination [17]. To overcome this issue, the bulk heterojunction was introduced in the 1990s by blending D and A together [6], forming an interpenetrating networking in an organic solvent so that an

exciton may have a greater chance of dissociation. As mentioned previously, this is the benchmark or baseline upon which we will build discussions of the engineering ingenuities implemented in the past two decades of OSCs research in this review. A standard heterojunction OSC example may consist of an active layer such as a poly(3-hexylthiophene) (P3HT) : [6,6]-phenyl-C_{61}-butyric acid methylester (PCBM) mix sandwiched between electrodes indium-tin oxide (ITO) and aluminum (Al) [6][18]. It is worth noting that fullerene derivatives such as PCBM, first introduced by Heeger et al, are incredibly efficient electron acceptors for photoexcited conjugated polymers with near unity quantum efficiency for exciton separation [19]. From the photovoltaic process described above, it is clear that the overall efficiency of an OSC follows Equation 1.

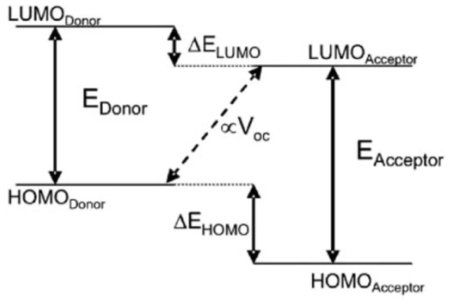

Figure 1. Energy level diagram within the active layer [6]

$$\eta_{net} = \eta_{absorption} \times \eta_{diffusion} \times \eta_{dissociation} \times \eta_{extraction}$$

(Equation 1)

To better understand the unique challenges faced by OSCs, it is conceptually beneficial to compare them against the commercially successful inorganic photovoltaic devices (IPDs). Due to its low bandgap of $1.1\ eV$, a silicon cell can absorb a continuous spectrum of light. In comparison, the most common OSC donor materials such as P3HT has a band gap of $1.9\ eV$ [20]. Upon excitation, IPDs produces free charge carriers instead of excitons. The former can transport freely thanks to the $p-n$ junction without the need for heterojunction-assisted electron-hole pair dissociation found in the latter. In addition, the former provides greater carrier mobility due to its rigid and crystalline structure while the latter relies on hopping transport. As a result, many IPDs can reach an AM1.5 PCE of 22% or higher, more than twice of that reported in the most cutting-edge OSCs which are limited by a theoretical conversion efficiency value of 15% [21][22]. Further, IPDs are more stable in a humid environment than OSCs [21]. It is worth noting that roughly 50% of the module cost in IPDs is due to the cost of silicon wafer production in spite of previous attempts to recycle rejected materials from the semiconductor industry [19]. Therefore, although OSCs may never surpass IPDs in efficiency, their competitiveness comes instead from the low production cost, low carbon footprint, high structural flexibility and high general applicability.

2.1 Absorption

The solar spectrum roughly fits that of black body radiation at $5900\ K$, ranging from ultraviolet to the infrared regions [19]. Bandgaps of $1.1\ eV$ and $2.0\ eV$ can absorb 77% and 30% of the solar irradiation respectively [23]. Thus, there exists great incentives in solar cell research to engineer low bandgap materials. Heterocycle monomers of benzodithiophene and carbazole rings are useful building blocks for such polymers with bandgaps as low as $1.0\ eV$ due to their coplanarity [23]. Introducing fluorine atoms to thienothiophenes and benzodithiophenes have also been observed to lower the HOMO energy level at roughly $0.1\ eV$ per repeating unit [23]. This has been attributed to its high electronegativity and low steric hinderance effect. Substituent grafting has also been demonstrated to be effective in tuning the material solubility, which in turn affects its HOMO level. For instance, the replacement of an alkyl side chain with an alkoxy group on a benzodithiophene unit decreased its HOMO by $0.1\ eV$ [23][24]. Although low bandgap materials may absorb a greater percentage of the solar spectrum, this does not equate to high energy utilization since electrons in low bandgap materials simply relax to the LUMO edge after excitation, generating significant thermal energy loss through lattice vibration. The truth is, a single heterojunction can only absorb a small window of the entire solar spectrum. The philosophy of Tandem solar cells is thus stacking multiple complementary absorbers to broaden the coverage.

Zhang et al constructed a Tandem cell made of a poly[(2,6-(4,8-bis(5-(2-ethylhexyl)thiophen-2-yl)-benzo[1,2-b:4,5-b′]dithiophene))-alt-(5,5-(1′,3′-di-2-thienyl-5′,7′-bis(2-ethylhexyl)benzo[1′,2′-c:4′,5′-c′]dithiophene-4,8-dione))] (PBDB-T) / F-M front sub-cell and a poly[4,8-bis(5-(2-ethylhexyl)thiophen-2-yl)benzo[1,2-b:4,5-b′]dithiophene-co-3-fluorothieno[3,4-b]thio-phene-2-carboxylate] (PTB7-Th) / NOBDT back sub-cell [25].

The HOMO and LUMO levels of the front cell was elevated through methyl substitution and the device showed a PCE of 10.08% with an open-circuit voltage (V_{OC}) of $0.98\ V$, a short-circuit current (J_{SC}) of $14.56\ mA\ cm^{-2}$ and a fill factor (FF) of 0.71 [25]. Within the $490{\sim}610\ nm$ domain, its external quantum efficiency (EQE) was over 70% [25]. The HOMO level of the back cell was elevated through electron-donating octyloxy incorporation and its LUMO level was lowered by fluorinization. The device showed a PCE of10.55% with a V_{OC} of $0.77\ V$, a J_{SC} of $19.16\ mA\ cm^{-2}$ and a fill factor of 0.70 [25]. Within the $630{\sim}750\ nm$ domain, its EQE was over 70% [25]. Using modelling based on the transfer matrix method, the simulation indicated that the PBDB-T/F-M and PTB7-Th/NOBDT layers should be $105\ nm$ and $100\ nm$ respectively [25]. Experimentally, this Tandem cell achieved an outstanding PCE of 14.11% with a V_{OC} of $1.71\ V$, a J_{SC} of $11.72\ mA\ cm^{-2}$

and an FF of 0.70 [25]. Tandem cells with a PCE greater than 10% have been rather common in the past decade, the trend is to move away from fullerene acceptors due to their weak absorptions and this also provide one additional degree of freedom for V_{OC} tuning [26][27][28].

The surface plasmonic effect, which takes place when the collective oscillation frequency of charges resonates with that of the incident electromagnetic field, may be used to increase photonic absorption. Duche et al. demonstrated light confinement using silver nanoparticles to achieve enhanced absorptance up to 50% [29]. Experimentally, the sample was fabricated by spin coating a colloidal solution of 40 nm silver nanoparticle to create a plasmon layer sandwiched between a silica substrate and a photoactive heterojunction of poly(2-methoxy-5-(20-ethyl-hexyloxy)-1,4-phenylenevinylene) (MEH-PPV)/PCBM [29]. Compared to the control sample, a maximum absorption gain at 500 nm was observed in the 375~800 nm spectral range [29]. Numerically, this result was confirmed using finite difference time domain (FDTD) simulation. For the calculation, each device was placed between two infinite sensors and illuminated with a plane wave at normal incidence. To solve the Maxwell's equations, the refractive indices of MEH-PPV/PCBM and the silver thin film were deduced and fitted from ellipsometry measurements using the Drude-Lorentz model [29]. Simulation showed that the stronger absorption could be attributed to preferential distribution of the electromagnetic field power density near the silver nanoparticles [29]. Min et al. reported a similar plasmon enhanced device. But they instead partially substituted the top transparent poly(3,4-ethylenedioxythiophene) (PEDOT) electrode with a periodic silver grating. Through varying the width, thickness and periodicity of the grating, the overall absorption improvement can be tuned to 50% under AM1.5 illumination [30].

The absorption efficiency of OSCs can also be improved through optical engineering. For instance, Tvingstedt et al. reported an echelle grating array that significantly increased the light path length by total internal reflection when it was laminated on the backside of a semitransparent solar cell using polydimethylsiloxane (PDMS) [31]. The device may be manufactured inexpensively by embossing an acrylic resin in a roll-to-roll process followed by silver metallization through thermal sublimation [31]. Paired with a semi-transparent solar cell such as 2:5 TQ1/PCBM70, the echelle reflector generates 24% more photocurrent under AM 1.5 solar irradiance [31]. At 700 nm wavelength closer to the band edge, the EQE was observed to be as much as 3.3 times that of the control group [31]. Moreover, when applied to a solar cell module, the echelle grating array was able to redirect light impinging on the dead area between cells to the photoactive region [31]. However, it is worth pointing out that experiments and simulation showed pronounced difference between the device-level and photoactive layer absorption, indicating the further optimization

needed to reduce parasitic loss [31]. A similar approach using pyramidal rear reflectors to enhance light harvesting was reported by Cao et al. The device consists of a silver-coated PDMS pyramidal structure with 30° base angles [32]. Due to its extended optical light path length, the P3HT/PCBM active layer showed a 75% increase in J_{SC} under AM 1.5 solar illumination [32]. Biology has also inspired researchers to design more efficient light absorbing layers. For example, Chen et al. reported a biomimetic nanostructure of periodic 180 nm deep grooves, templated from moth eyes, which are perfect sub-wavelength anti-reflective structures with great transmittance throughout the entire visible spectrum [33]. The device was fabricated by UV-assisted nanoimprinting lithography and yielded a 24.3% increase in J_{SC} without comprising its V_{OC} under AM 1.5 [33]. Maxwell coupled wave analysis attributed the improvement to the refractive index gradient from the moth-eye nanostructure. In addition, nanostructure surface was super-hydrophobic with contact angles around 150° [33]. As a consequence, the device is essentially self-cleaning, meaning that it will be able to block moisture and dust from accumulating on the cell surface in a real environment [33].

2.2 Diffusion

The second crucial factor in improving the PCE of OSCs is $\eta_{diffusion}$. As a general rule of thumb, it is beneficial to increase the diffusion length of excitons so that there is a greater probability that they will make it to a D/A interface, where dissociation occurs. Exciton diffusion in organic semiconductors is a macroscopic phenomenon of its underlying Förster-mediated random energy transfer process as a result of strong exciton-phonon interaction in the weak dipole-dipole coupling limit. Equation 2 for singlet exciton diffusion length is shown below where κ, Φ_F, σ, n and a are the dipole orientation factor, fluorescence quantum yield, Förster integral overlap, refractive index and average hopping distance respectively [34][35]. However, the evaluation of diffusion length remains challenging as it is often complicated by factors whose influences are only understood on an experimental level such as grain boundaries and packing geometry. As an example, to illustrate the importance of grain boundaries, Lunt et al. demonstrated experimentally that diffusion length of 3,4,9,10-perylenetetracarboxylic dianhydride (PTCDA) is limited by non-radiative losses at grain boundaries, whose quenching rate can be $\sim 10^4$ higher than other pathways in single crystals [34]. However, a sufficiently large grain diameter ~ 20 times that of single crystals no longer exhibits boundary quenching according to the same model [34]. Similar research from Sim et al. suggested that high crystalline order reduced the inter-chromophore distance which enhanced Förster energy transfer process as a consequence [36]. One recent novel method reported for photoactive layer morphology control is crystalline molecular templating. Zhao

et al. demonstrated a pentacene templated $20\ nm$ lead phthalocyanine (PbPC) / $40\ nm$ C_{60} solar cell which demonstrated a 48% increase in J_{SC} compared to the control group [37]. On the other hand, the research of Rim et al. showed that, with identical grain sizes, the EQE and diffusion length of *trans*- 3,4,9,10- perylene tetracarboxylic bisbenzimidazole (PTCBI) are respectively 30% and 43% higher than those of *cis*-PTCBI due to more compact molecular packing [38].

$$L_D = \sqrt{\frac{\kappa^2 \Phi_F \sigma}{8\pi n^4 a^4}}$$

(Equation 2)

2.3 Dissociation

As outlined in the opening paragraph, if an exciton reaches the interface before recombination occurs and the D/A energy mismatch renders dissociation energetically favorable, then the electron and hole form a charge transfer state with the electron on the acceptor and the hole on the donor. Even after an exciton dissociates at the D/A interface, the electron is still technically coulombically attracted to the hole. If the electron loses kinetic energy due to scattering, then the electron-hole pair will be trapped at the interface. To prevent this from happening, it is recommended to have $LUMO_D$ $50\sim100\ meV$ higher than $LUMO_A$ [17]. Many researchers have resorted to the Onsager-Braun formulism to devise a precise relation for charge separation efficiency. However, many systems simply do not exhibit the field or temperature dependencies outlined in the model [16]. Some have suggested the delocalization of holes along polymer chains to be the underlying mechanism for Coulomb attraction reduction which eventually leads to geminate pair separation. The conceptualization of this theory is aided by the observations that acceptors are commonly fullerene derivatives where electrons are considered "captured" and donors are commonly polymers like P3HT where holes have to freedom to "hop around" [39]. Arkhipov et al. proposed a model where dissociation is simplified to an exciton in a dipolar interface, equidistant with fullerene acceptor on one side and layers of polymer donor chains on the other. Further, Arkhipov suggested that if the effective hole energy on the outer polymer chains were lower than those of their inner counterparts, then dissociation could take place [40][41]. With J available polymer layers, the dissociation probability under electric field F in the 1D nearest-neighbor hopping regime can be expressed by Equation 3 below, where τ is the recombination lifetime and υ is the hopping rate governed by the Miller-Abrahams equations [39][42]. $p(F)$ may be considered a theoretical equivalent for $\eta_{dissociation}$.

$$p(F) = \left[1 + \frac{1}{\tau}\sum_{j=1}^{J-1} \frac{1}{\nu_{j\to j+1}(F)} e^{\frac{\Delta E_{1\to j}(F)}{k_B T}}\right]^{-1}$$

(Equation 3)

At the D/A interface, energy loss always occurs, through both radiative and non-radiative recombination pathways. This is reflected in $E_{CT} - eV_{OC}$, where E_{CT} is the energy difference between the D ionization potential and the A electron affinity. Within the Shockley-Queisser framework, detailed balance analysis has shown that nearly all solar cells intrinsically lose $\sim 0.3\ eV$ due to radiative recombination [43]. On the other hand, structural defects, interface morphology and energetic traps are known to contribute further to non-radiative recombination [43]. For example, Ran et al. suggested the non-radiative recombination rate to be a function of molecular orientation and face-on interfaces had been observed to have better performance than their edge-on counterparts [44]. The effect of interface on dissociation efficiency is further confirmed by Ojala et al., who showed glass transition temperature annealing led to donor film roughness improvement, resulting in a 2.2-fold increase in FF of the merocyanine/C_{60} device [45].

2.4 Extraction

In OSCs, charge motion relies on thermally activated hopping where the electron and hole mobility values are significantly lower than those of band transport observed in inorganic semiconductors. This is sometimes referred to as the Poole-Frenkel effect [46]. Under realistic operating conditions, steady state mobilities can successfully describe the characteristics of OSCs. Having said that, it is worth noting that within the first few nanoseconds after a laser light pulse, high energy carriers, that are excited to the upper part of the DOS before thermalization loss, may access fast diffusion routes for extraction. Le Corre et al. demonstrated that the current dispersion played a limited role in charge extraction; that is to say, drift and diffusion remained valid framework for understanding charge carrier extraction as shown in Equation 4 [47].

$$f^{extraction} = f^{drift} + f^{diffusion} = \frac{2\mu V_{effective}}{L^2_{active\ layer}} + \frac{8\mu k_B T}{qL^2_{active\ layer}}$$

(Equation 4)

For free carriers, non-geminate pathways via bi-molecular and trap-assisted recombination become the leading causes for a reduced $\eta_{extraction}$ [16]. The former can be described by Langevin formalism which states that charge recombination is proportional to the likelihood that an electron and a hole encounter each other within the Coulombic radius. Hence it may be roughly approximated to the product of carrier concentrations and relative mobility [48]. This explains the reason behind the rapid FF decrease when the photoactive layer thickness exceeds $150\ nm$. Scharber et al. demonstrated that modification of the carbon bridging atom in polymer poly[2,6-(4,4-bis-(2-ethylhexyl)-4H-cyclopenta[2,1-b;3,4-b′]dithiophene)-*alt*-4,7(2,1,3-benzothiadiazole)] (PCPDTBT) to silicon was able to significantly reduce the

bimolecular recombination coefficient [49]. Venkatesan et al. showed applying a simple nitrobenzene solvent additive was effective creating a shaper interface between P3HT and $PC_{60}BM$, leading to lower bimolecular recombination [50]. The trap-assisted process described above is more involved in comparison, where defects or impurities create energy levels within the forbidden band gap to capture free carriers for recombination. For instance, in poly(p-phenylene vinylene) (PPV) derivatives, electron traps typically have density of $2 \times 10^{17}\ cm^{-3}$ and follow a Gaussian distribution centered around $0.7{\sim}0.8\ eV$ below the LUMO [51]. By contaminating merely 1% of PCBM (LUMO: $3.7\ eV$) with a stronger electron acceptor 7,7,8,8-tetracyanoquinodimethane (TCNQ) (LUMO: $4.5\ eV$), Mandoc showed that the PCE and FF of a standard PPV/PCBM blend decreased from 2.0% to 0.6% and 52% to 42% respectively [52]. This experiment proves that the elimination of deep traps is an essential condition for high performance OSCs.

To increase $\eta_{extraction}$, electron and hole extraction layers, in contact with cathode and anode respectively, have been devised to provide better energy matching and interlayer adhesion. The most well-known hole extraction layer is PEDOT:PSS. However, recent research has pivoted from the ITO corrosive PEDOT:PSS to transition metal oxides for performance stability. Gu et al. demonstrated a solution-processible ultrathin MoS_2 nanosheet-based hole extraction layer for P3HT:$PC_{61}BM$ with PCE of 8.11% [53]. The layer has a hole mobility value of $200\ cm^2\ V^{-1}\ S^{-1}$ and its $-80\ mV$ energy offset from D reinforces the built-in potential through an induced dipole moment, which facilitate hole extraction [53]. Other common hole extraction layers that have been reported include V_2O_5, WO_3 and NiO_x [54][55][56]. Similarly, common electron extraction layers are SnO_x, TiO_x and ZnO, which all share the attributes of optical transparency, high electron mobility and inexpensive processing conditions. It is worth noting that TiO_x can decompose water through photocatalysis upon thermal activation and thus may result in devices with compromised stability under humid conditions [57][58].

Although bulk heterojunction design has remained the focus of this report thus far, it is important to realize its intrinsic structural flaw. For carrier collection, continuous pathway percolation is often difficult to guarantee due to the random phase separation of D and A materials. To address this issue, interdigitated heterojunction fabrication through electrode templating, self-assembly and nanoimprinting has attracted research attention. For instance, Hu et al. demonstrated nanoscale dimensionality control over diameters, heights and spacings in fabricating P3HT pillar arrays using an anodic aluminum oxide template. This technique is particularly attractive for practical device manufacturing whose area requirement usually exceed $100\ mm^2$ [59].

3.0 Circuit Model of OSCs

This section aims to briefly examine OSC efficiency from the circuit modelling perspective and at the same time elucidate origin of the key metrics often reported in OSC journals. The tools for quantitatively estimating energy loss enables targeted optimization and hopefully helps the readers develop the mathematical intuition for trouble shooting low performance OSC devices through this process.

The current response as a function of the applied bias may be modelled by Equation 5 and a typical current-voltage characteristic is shown in Figure 2. I_0 and I_L are the dark current and photocurrent respectively, R_S and R_{SH} are the series resistance and shunt resistance respectively. To maximize PCE is to maximize the product of J_{SC} and V_{OC}, as well as FF as shown in Equation 6 and 7 [60].

$$I = I_0 \cdot \left(e^{\frac{e}{nk_BT}(V-IR_S)} - 1\right) + \frac{V-IR_S}{R_{SH}} - I_L$$

(Equation 5)

$$FF = \frac{P_{max}}{J_{sc}V_{oc}}$$

(Equation 6)

$$PCE = \frac{P_{max}}{\Phi_C} = J_{SC} \times V_{OC} \times FF \Big/ \Phi_C$$

(Equation 7)

FF is a measure of the squareness of the current-voltage characteristic curve and can be pushed further towards 100% by decreasing R_S and increasing R_{SH}. In an efficient donor acceptor system, that is, an OSC with ohmic electrical contact and predominantly biomolecular recombination, the ratio of the recombination and extraction rate is an excellent predictor for FF. Based on experimental data collected from polymer fullerene and small molecule devices as well as drift-diffusion simulation, Bartesaghi et al. devised a metric θ to model the competition between the aforementioned two rates. As shown in Equation 8, γ is the strength of bimolecular recombination, $V_{internal}$ is the internal voltage approximately V_{OC} at one sun, L is the active layer thickness, G is the volume generation rate of the free carriers, μ_n and μ_p are the mobility of electrons and holes respectively [60]. The parameters could be obtained from time-delayed collection field measurements or copied from existing literature. θ shares an inversely proportional relationship with FF of the range from 0.26 to 0.74. In addition, Bartesaghi et al. has demonstrated its power to explain why lower light intensity or active layer thickness leads to higher FF values in a systematic fashion [60].

$$\theta \propto \frac{k_{recombination}}{k_{extraction}} = \frac{\gamma G L^4}{\mu_n \mu_p V_{internal}^2}$$

(Equation 8)

R_S is a lumped term accounting for all series resistance contributions in the device architecture from bulk transport to line loss. For bulk transport, increasing and decreasing the area and thickness of a photoactive layer respectively may decrease the overall bulk resistance, but at the same time, this inevitably raises the sheet layer power loss

and lowers absorption [61]. For line loss, silver and copper are often used as electrical contacts due to their high conductivities. Having said that, process compatibility also plays an important role in contact material selection such as the case of active layer impurity from copper diffusion [62]. On the other hand, R_{SH}, ideally infinite, may become finite due to defects that allow parasitic leakage current to pass through. V_{OC} is a sensitive function of the energy levels of the photovoltaic materials, as well as the engineering of interfaces and contacts. Specifically, it is affected by the cathode anode work function difference and the $HOMO_D/LUMO_A$ difference [63]. Finally, improvement in J_{SC} can be achieved by adopting lower bandgap materials preferably with a more ordered molecular arrangement, a broader absorbable spectrum and a higher transport mobility [64]. It is worth noting that the central assumption in the circuit model of OSCs is that the photocurrent I_L stays constant under a given incident light intensity and independent of the externally applied voltage, as shown in Figure 3 [65]. In other words, this means that the dark current J_{SC} at V_{OC} cancel each other out, which does not hold true for most OSCs as pointed out by Mazhari et al. using the blend MEH-PPV/PCBM OSC as an example to substantiate the need for a more sophisticated circuit model [65].

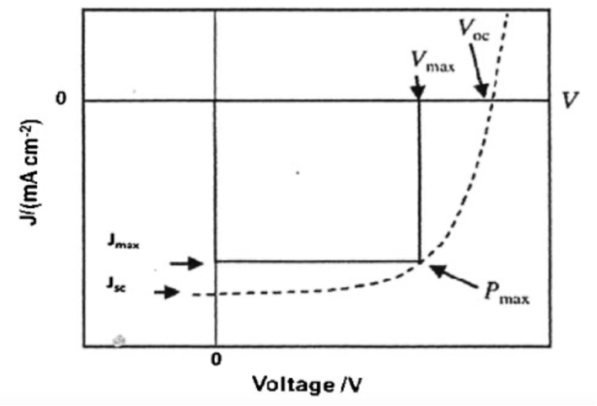

Figure 2. A typical current-voltage characteristic of a photovoltaic device [64]

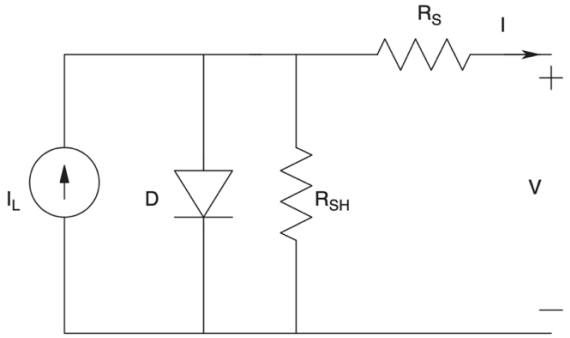

Figure 3. Conventional OSC circuit model [65]

4.0 Non-binary/Hybrid Bulk Heterojunction

The promise of clean energy through affordable bulk heterojunction OSCs, the devices that have been the focus of this review so far, was initiated by the discovery of efficient electron transfer from polymers to buckminsterfullerene in 1992 [66]. Since then, enormous efforts have been devoted to optimizing photoactive layer bandgap, material processability and device architecture, as well as understanding the fundamental physics

that govern the operation of OSCs. Decades of research has rendered OSCs with a PCE greater than 10% a common sight, finally cost effective and commercially competitive [66]. In 2011 Germany, the price of PV electricity for private households was approximately $0.25\,€/kWh$, compared to its hydro-, coal- or gas-powered plant counterparts at below $0.10\,€/kWh$ [67]. Recent exploration of non-fluorene based acceptors has yielded record-breaking PCE of 16% in PM6/Y6 heterojunction, which further confirms the potential of OSCs as a feasible mean for sustainable energy generation [68]. Having said that, under the second thermodynamics law limit, Giebink et al. derived the theoretical maximum efficiency values to be 27% and 22% for OSCs with 0.3 eV and 0.5 eV free energy respectively for efficient charge transfer [69]. This is significantly less than the commonly quoted 31% efficiency under the Shockley-Queisser limit due to non-negligible exciton binding energy and unavoidable loss at the heterojunction [69]. To get closer to this limit, this section will shift the focus away from the traditional polymer-fullerene-based device and place more emphasis on other recent novel approaches devised to further increase the OSC efficiency.

In polymer-fullerene-based OSCs, the acceptors contribute little to the light absorption. Thus, it would be beneficial to identify or engineer a new material that has an absorption spectrum complementary to D without compromising the electron transfer efficiency. Regrettably, such materials remain elusive and little progress has been made in engineering it. An alternative approach is to mix two or more donor materials with complementary absorption spectrums, like in the P3HT:CuPc/PCBM design [70]. Further, it would be greatly beneficial to be able to utilize incident photons that are above and below the donor bandgap. In the former case, tetracene and pentacene have been proven effective materials for thermal loss reduction due to their fission property, a process in which one singlet exciton of higher energy is converted into two triplet excitons of lower energy [71][72]. Absorption deficiency in the latter case may be addressed through up-conversion. Rare earth metal ions have been shown to be effective in converting sub-bandgap infrared photons. For instance, Yb^{3+} doped hole extraction layer MoO_3 has been demonstrated to increase the $900\sim1000\,nm$ absorption in a P3HT:PCBM system [73]. In addition, metal-organic chromophore sensitizers with strong spin orbital coupling can also absorb lower energy photons and form triplet excitons through intersystem crossing. These triplets can then form intermediate pairs that eventually convert to singlet excitons through triplet-triplet annihilation [74].

As discussed previously, one of the major driving forces that has been pushing the development of OSCs over its far more energy efficient inorganic rivals is affordability, due to the excellent low-temperature solution-based processability of photoactive organic compounds. Although the primary focus of review has been to address the

question of "How can we make OSCs more efficient?", it is worthwhile to consider the other perspective "How can we make Si solar cells cheaper?". Indeed, the question of "Can we get the best of both worlds?" has led to the development of organic/inorganic hybrid systems. Particularly, quantum dots are excellent acceptor candidates as their absorption can be tuned to cover a broad spectral range. In addition, they have high electron mobility and photochemical stability. Ren et al. demonstrated a novel method to bound CdS quantum dots onto crystalline P3HT nanowires (PCE ~ 3.5%) through solvent-assisted grafting and ligand exchange [75]. This technique allows quantum dots to take advantage of the solution processability from polymers and promotes the formation of percolation network [75]. Various degrees of PCE enhancement have been reported for other P3HT/QT hybrid systems: ~2% in GaAs, ~2% in CdSe, ~1% in PbS [76][77][78]. On the other hand, to mix more elements from OSCs into the Si system, PCE of ~10% has been obtained from Si/P3HT and Spiro-OMeTAD hybrid cells, followed by 9% in PEDOT:PSS/SiNWs and 3.5% in polyaniline/n-Si [79][80][81][82]. To ensure smooth charge transfer in a hybrid system, the interface must be treated with excessive care to deliver performance consistency. For instance, Rusli et al. demonstrated that in a PEDOT/Si hybrid cell, oxygen-terminated Si surface facilitated favorable band alignment whereas hydrogen-terminated Si surface blocked the internal electrical field [83]. Further, if the native SiO_x is too thick, it can reduces V_{OC} and FF [83].

5.0 Life Cycle Analysis

To ensure that OSCs do not create new environmental issues, life cycle assessment (LCA) is usually conducted to evaluate the energy footprint from raw material acquisition, device production to the eventual waste disposal. Using the P3HT:C_{60}PCBM bulk heterojunction as an example, the embodied energy for pyro-tetralin C_{60}PCBM and P3HT is $65\ GJ/kg$ and $2020\ MJ/kg$ respectively [84]. Given that fullerenes are usually modified to methano-fullerenes for solubility and electrical property optimization, the amount of waste generated per product mass is likely much higher than the reported value here. Similarly, polymer engineering, such as alkyl substitution and backbone fluorination, commonly used to change the absorption spectrum and hole mobility will undoubtedly add to the total energy cost. Following the guideline for photovoltaics LCA, the annual solar energy, performance ratio and grid efficiency are assumed to be $1700\ kWh/m^2$, 75% and 31% respectively [84]. For a 5% $250\ cm^2$ $12.5\ mg\ P3HT/10.0\ mg\ C_{60}PCBM$ system, Anctil et al. calculated that the primary energy would be $\sim 4\ MJ/W_p$, much less than $\sim 25\ MJ/W_p$ for $mc-Si$ solar cells [84]. Further, the EPT was reported to be roughly 0.28 years [84].

Besides increasing PCE of the devices, which has been the focus of this review, two other ways to reduce the EPT are to adopt a synthesis plan based on green chemistry and to design recyclable OSCs. Green chemistry refers to a type of reaction methodology of low energy, at low cost and with minimal production of toxic waste. Applying this to the production of polymer donors, the definition translates to favoring polymerization reactions that evolve water as a by-product and use bio-feedstock derived compounds as the starting materials. Burke et al. have written a comprehensive review on the subject [85]. For instance, the direct heteroarylation polymerization (DHAP) has been proposed as a greener alternative to the Stille process for the synthesis of P3HT [85]. In comparison, the former spares the lithiation and stannylation steps in the latter while achieving 98% regioregularity with $M_n \sim 30\ kDa$ and 99% yield in THF, under the proper loading of one and two mole percent of Herrmann catalyst and phosphine ligand respectively [85]. Given that it has been estimated by Osedach et al. that the purification contributes to $\sim 50\%$ of the laboratory-scale synthesis cost for P3HT, it is evident that DHAP is a substantially more economical route [85]. Meanwhile, Zhou et al. demonstrated a recyclable OSC on a biodegradable free-standing cellulose nanocrystal substrate to replace the traditional petroleum-based substrates [86]. The cellulose substrate can be re-dispersed when immersed in water and the photoactive organic layers can be separated in an organic solvent, leaving behind the metal electrodes to be filtered out. Although the PBDTTT-C:PCBM based device only had an average PCE of 2.7%, the cellulose OSCs could have an overreaching impact for the sustainability of printed electronics given preparation method used [86].

ERF, defined as the ratio between the total energy saved during a product's lifetime and the energy that was put in to create the product in the first place, is also an important metric in photovoltaics research. Essentially, the ERF informs the public how much extra energy is gained from an OSC device. Evidently, given a set combination of PCE and energy input, a longer operational lifetime will result in a greater ERF. To truly qualify as affordable, Barbec et al. argued that the market-entry lifetime should be $3 \sim 5$ years based on the usability of electronic goods that OSCs can potentially power [87]. With the goal of device longevity in mind, it is imperative to understand the degradation kinetics of OSCs. In a typical benchmark P3HT:PCBM system, the nanoscale morphology of interpenetrating D/A materials alters above the glass transition temperature. The nucleation and diffusion of PCBM grow micron-scale clusters and diminish the interface area following the kinetics of Ostwald ripening [88]. This manifests itself as a significant reduction in I_{SC}, as modelled by Equation 9 and 10 below. From fitting, researchers may predict the lifetime of OSC devices in a quantitative manner [88]. Another known factor that contributes to OSC degradation is humidity ingress. Kawano et al.

showed water adsorption resulted in spatially inhomogeneous resistivity increase at This is further confirmed by Fecher et al., who measured the activation energy for water diffusion to be $43\ kJ\ mol^{-1}$ in a P3HT:PCBM system and called for more research into humidity proof hole extraction layer materials such as MoO_x to replace PEDOT:PSS [90]. Further, they demonstrated that a shelf life of 100,000 hours was achieved at $65℃\ 85\%\ RH$ when using a $9.3\ cm$ wide adhesive rim for protective packaging and confirmed that the water diffusion behaviour follows Fick's Law of diffusion [90]. A comprehensive review on OSC degradation through various means including polymer photo-oxidation and electrode etching was published by Jorgensen et al. in 2008 [91]. Although slightly outdated, the degradation principles should stay the same. In addition, the characterization methods section offers practical information invaluable for investigating degradation in OSCs; thus it is highly recommended for readers who wish to delve deeper into this topic [91].

$$I_{SC}(t) = I_{SC}(\infty) + I_{SC}(0)e^{-k'_{degradation}\sqrt{t}}$$

(Equation 9)

$$k'_{degradation} = Ae^{-E_a/k_BT}$$

(Equation 10)

PEDOT:PSS layer and blend interface due to the formation of insulating patches [89].

6.0 Summary

This report reviewed the emerging technology of polymer/fullerene-based bulk heterojunction OSCs. Specifically, the theoretical models concerning the fundamental four steps of photovoltaic process: absorption, diffusion, dissociation and extraction were examined, and the latest engineering ingenuities devoted to improving their efficiencies were discussed. The author believes that bandgap engineering, morphology control and interface optimization will remain the most crucial aspects for achieving $> 10\%$, near 15% or even higher efficiency in OSCs. Research into green chemistry and degradation pathways is less frequently reported in the largely efficiency focused literature, but nevertheless crucial for the successful commercialization of OSCs. Further, given the advantage of inorganic photovoltaic devices over OSCs in terms of efficiency, the author believes that current research should emphasize on the main appeals of OSCs, which are affordability, processability and applicability. To become truly market competitive, it is possible that future OSCs will need to move past the binary bulk heterojunction paradigm to overcome its inherent limitations; thus, the report also dedicated a section on OSCs with non-binary or hybrid designs.

References

[1] E. Dans, “In A Post-Pandemic World, Renewable Energy Is The Only Way Forward,” *Forbes*. [Online]. Available: https://www.forbes.com/sites/enriquedans/2020/05/03/in-a-post-pandemic-world-renewable-energy-is-the-only-wayforward/#ae9a1ca17b6f. [Accessed: 24-May-2020].

[2] A. Mohammad Bagher, “Comparison of Organic Solar Cells and Inorganic Solar Cells,” *Int. J. Renew. Sustain. Energy*, vol. 3, no. 3, p. 53, 2014.

[3] Z. Dobrotkova, K. Surana, and P. Audinet, “The price of solar energy: Comparing competitive auctions for utility-scale solar PV in developing countries,” *Energy Policy*, vol. 118, pp. 133–148, Jul. 2018.

[4] E. Dans, “What The Post-Pandemic World Needs Is A Solar Energy Revolution,” *Forbes*, 21-May-2020. [Online]. Available: https://www.forbes.com/sites/enriquedans/2020/05/21/what-the-post-pandemic-world-needs-is-a-solar-energy-revolution/#46dc6afa151e. [Accessed: 24-May-2020].

[5] J. C. Bernède, “Organic photovoltaic cells: History, principle and techniques,” *Journal of the Chilean Chemical Society*, vol. 53, no. 3. Sociedad Chilena de Quimica, pp. 1549–1564, 2008.

[6] R. P. Singh and O. S. Kushwaha, “Polymer Solar Cells: An Overview,” *Macromol. Symp.*, vol. 327, no. 1, pp. 128–149, May 2013.

[7] T. Liu *et al.*, “Ternary Organic Solar Cells Based on Two Compatible Nonfullerene Acceptors with Power Conversion Efficiency >10%,” *Adv. Mater.*, vol. 28, no. 45, pp. 10008–10015, Dec. 2016.

[8] J. Zhao *et al.*, “Efficient organic solar cells processed from hydrocarbon solvents,” *Nat. Energy*, vol. 1, no. 2, pp. 1–7, Feb. 2016.

[9] O. K. Simya, P. Radhakrishnan, A. Ashok, K. Kavitha, and R. Althaf, “Engineered nanomaterials for energy applications,” in *Handbook of Nanomaterials for Industrial Applications*, Elsevier, 2018, pp. 751–767.

[10] M. Kaltenbrunner *et al.*, “Ultrathin and lightweight organic solar cells with high flexibility,” *Nat. Commun.*, vol. 3, no. 1, pp. 1–7, Apr. 2012.

[11] C. Heald, “New solar power source and storage developed,” *BBC NEWS*, 2020. [Online]. Available: https://www.bbc.com/news/science-environment-50717446. [Accessed: 13-Jul-2020].

[12] J. Li, “Solarmer Energy, Inc. Breaks Psychological Barrier with 8.13% OPV Efficiency | Business Wire,” *BusinessWire*, 2010. [Online]. Available: https://www.businesswire.com/news/home/20100727005484/en/Solarmer-Energy-Breaks-Psychological-Barrier-8.13-OPV. [Accessed: 13-Jul-2020].

[13] T. Soga, “Fundamentals of Solar Cell,” *Conversion*, pp. 3–43, Jan. 2006.

[14] A. Bagga, P. K. Chattopadhyay, and S. Ghosh, “Origin of Stokes shift in InAs and CdSe quantum dots: Exchange splitting of excitonic states,” *Phys. Rev. B - Condens. Matter Mater. Phys.*, vol. 74, no. 3, p. 035341, Jul. 2006.

[15] P. Ewart, “Selection rules,” in *Atomic Physics*, Morgan & Claypool Publishers, 2019, pp. 3–7.

[16] C. M. Proctor, M. Kuik, and T. Q. Nguyen, “Charge carrier recombination in organic solar cells,” *Progress in Polymer Science*, vol. 38, no. 12. Pergamon, pp. 1941–1960, 01-Dec-2013.

[17] P. Würfel, “Photovoltaic principles and organic solar cells,” *Chimia (Aarau).*, vol. 61, no. 12, pp. 770–774, 2007.

[18] M. Girtan and M. Rusu, “Role of ITO and PEDOT:PSS in stability/degradation of polymer:fullerene bulk heterojunctions solar cells,” *Sol. Energy Mater. Sol. Cells*, vol. 94, no. 3, pp. 446–450, Mar. 2010.

[19] A. Goetzberger, C. Hebling, and H. W. Schock, “Photovoltaic materials, history, status and outlook,” *Materials Science*

and Engineering R: Reports, vol. 40, no. 1. Elsevier Ltd, pp. 1–46, 01-Jan-2003.

[20] Z. Genene *et al.*, "High Bandgap (1.9 eV) Polymer with Over 8% Efficiency in Bulk Heterojunction Solar Cells," *Adv. Electron. Mater.*, vol. 2, no. 7, p. 1600084, Jul. 2016.

[21] N. Yeh and P. Yeh, "Organic solar cells: Their developments and potentials," *Renewable and Sustainable Energy Reviews*, vol. 21. Elsevier Ltd, pp. 421–431, 01-May-2013.

[22] A. W. Blakers, A. Wang, A. M. Milne, J. Zhao, and M. A. Green, "22.8% efficient silicon solar cell," *Appl. Phys. Lett.*, vol. 55, no. 13, pp. 1363–1365, Sep. 1989.

[23] T. Xu and L. Yu, "How to design low bandgap polymers for highly efficient organic solar cells," *Materials Today*, vol. 17, no. 1. Elsevier B.V., pp. 11–15, 01-Jan-2014.

[24] W. Li, Y. Wu, X. Li, Y. Xie, and W. Zhu, "Absorption and photovoltaic properties of organic solar cell sensitizers containing fluorene unit as conjunction bridge," *Energy Environ. Sci.*, vol. 4, no. 5, pp. 1830–1837, May 2011.

[25] Y. Zhang *et al.*, "Nonfullerene Tandem Organic Solar Cells with High Performance of 14.11%," *Adv. Mater.*, vol. 30, no. 18, May 2018.

[26] Y. Cui *et al.*, "Fine-Tuned Photoactive and Interconnection Layers for Achieving over 13% Efficiency in a Fullerene-Free Tandem Organic Solar Cell," *J. Am. Chem. Soc.*, vol. 139, no. 21, pp. 7302–7309, May 2017.

[27] G. Liu *et al.*, "15% Efficiency Tandem Organic Solar Cell Based on a Novel Highly Efficient Wide-Bandgap Nonfullerene Acceptor with Low Energy Loss," *Adv. Energy Mater.*, vol. 9, no. 11, p. 1803657, Mar. 2019.

[28] S. Chen *et al.*, "A Nonfullerene Semitransparent Tandem Organic Solar Cell with 10.5% Power Conversion Efficiency," *Adv. Energy Mater.*, vol. 8, no. 31, p. 1800529, Nov. 2018.

[29] D. Duche *et al.*, "Improving light absorption in organic solar cells by plasmonic contribution," *Sol. Energy Mater. Sol. Cells*, vol. 93, no. 8, pp. 1377–1382, Aug. 2009.

[30] C. Min, J. Li, G. Veronis, J. Y. Lee, S. Fan, and P. Peumans, "Enhancement of optical absorption in thin-film organic solar cells through the excitation of plasmonic modes in metallic gratings," *Appl. Phys. Lett.*, vol. 96, no. 13, p. 133302, Mar. 2010.

[31] K. Tvingstedt, Z. Tang, and O. Inganäs, "Light trapping with total internal reflection and transparent electrodes in organic photovoltaic devices," *Appl. Phys. Lett.*, vol. 101, no. 16, p. 163902, Oct. 2012.

[32] W. Cao, J. D. Myers, Y. Zheng, W. T. Hammond, E. Wrzesniewski, and J. Xue, "Enhancing light harvesting in organic solar cells with pyramidal rear reflectors," *Appl. Phys. Lett.*, vol. 99, no. 2, p. 023306, Jul. 2011.

[33] J.-D. Chen *et al.*, "Enhanced Light Harvesting in Organic Solar Cells Featuring a Biomimetic Active Layer and a Self-Cleaning Antireflective Coating," *Adv. Energy Mater.*, vol. 4, no. 9, p. 1301777, Jun. 2014.

[34] R. R. Lunt, J. B. Benziger, and S. R. Forrest, "Relationship between crystalline order and exciton diffusion length in molecular organic semiconductors," *Adv. Mater.*, vol. 22, no. 11, pp. 1233–1236, Mar. 2010.

[35] M. Yang and G. R. Fleming, "Influence of phonons on exciton transfer dynamics: comparison of the Redfield, Förster, and modified Redfield equations," *Chem. Phys.*, vol. 282, no. 1, pp. 163–180, Aug. 2002.

[36] M. Sim *et al.*, "Dependence of exciton diffusion length on crystalline order in conjugated polymers," *J. Phys. Chem. C*, vol. 118, no. 2, pp. 760–766, Jan. 2014.

[37] W. Zhao, J. P. Mudrick, Y. Zheng, W. T. Hammond, Y. Yang, and J. Xue, "Enhancing photovoltaic response of organic solar cells using a crystalline molecular template," *Org. Electron.*, vol. 13, no. 1, pp. 129–135, Jan. 2012.

[38] S. B. Rim, R. F. Fink, J. C. Schöneboom, P. Erk, and P. Peumans, "Effect of

molecular packing on the exciton diffusion length in organic solar cells," *Appl. Phys. Lett.*, vol. 91, no. 17, p. 173504, Oct. 2007.

[39] M. Wiemer, M. Koch, U. Lemmer, A. B. Pevtsov, and S. D. Baranovskii, "Efficiency of exciton dissociation at internal organic interfaces beyond harmonic approximation," *Org. Electron.*, vol. 15, no. 10, pp. 2461–2467, Oct. 2014.

[40] V. I. Arkhipov, P. Heremans, and H. Bässler, "Why is exciton dissociation so efficient at the interface between a conjugated polymer and an electron acceptor?," *Appl. Phys. Lett.*, vol. 82, no. 25, pp. 4605–4607, Jun. 2003.

[41] V. I. Arkhipov and H. Bässler, "Exciton dissociation and charge photogeneration in pristine and doped conjugated polymers," *Phys. Status Solidi Appl. Res.*, vol. 201, no. 6, pp. 1152–1187, May 2004.

[42] A. Miller and E. Abrahams, "Impurity conduction at low concentrations," *Phys. Rev.*, vol. 120, no. 3, pp. 745–755, Nov. 1960.

[43] S. M. Menke, N. A. Ran, G. C. Bazan, and R. H. Friend, "Understanding Energy Loss in Organic Solar Cells: Toward a New Efficiency Regime," *Joule*, vol. 2, no. 1. Cell Press, pp. 25–35, 17-Jan-2018.

[44] N. A. Ran *et al.*, "Impact of interfacial molecular orientation on radiative recombination and charge generation efficiency," *Nat. Commun.*, vol. 8, no. 1, pp. 1–9, Dec. 2017.

[45] A. Ojala *et al.*, "Merocyanine/C60 Planar Heterojunction Solar Cells: Effect of Dye Orientation on Exciton Dissociation and Solar Cell Performance," *Adv. Funct. Mater.*, vol. 22, no. 1, pp. 86–96, Jan. 2012.

[46] J. Frenkel, "On pre-breakdown phenomena in insulators and electronic semi-conductors [3]," *Physical Review*, vol. 54, no. 8. American Physical Society, pp. 647–648, 15-Oct-1938.

[47] V. M. Le Corre, A. R. Chatri, N. Y. Doumon, and L. J. A. Koster, "Charge Carrier Extraction in Organic Solar Cells Governed by Steady-State Mobilities," *Adv. Energy Mater.*, vol. 7, no. 22, p. 1701138, Nov. 2017.

[48] G. Lakhwani, A. Rao, and R. H. Friend, "Bimolecular Recombination in Organic Photovoltaics," *Annu. Rev. Phys. Chem.*, vol. 65, no. 1, pp. 557–581, Apr. 2014.

[49] T. M. Clarke *et al.*, "Significantly Reduced Bimolecular Recombination in a Novel Silole-Based Polymer: Fullerene Blend," *Adv. Energy Mater.*, vol. 1, no. 6, pp. 1062–1067, Nov. 2011.

[50] S. Venkatesan *et al.*, "Critical role of domain crystallinity, domain purity and domain interface sharpness for reduced bimolecular recombination in polymer solar cells," *Nano Energy*, vol. 12, pp. 457–467, Mar. 2015.

[51] M. Kuik, L. J. A. Koster, G. A. H. Wetzelaer, and P. W. M. Blom, "Trap-assisted recombination in disordered organic semiconductors," *Phys. Rev. Lett.*, vol. 107, no. 25, p. 256805, Dec. 2011.

[52] M. M. Mandoc, F. B. Kooistra, J. C. Hummelen, B. De Boer, and P. W. M. Blom, "Effect of traps on the performance of bulk heterojunction organic solar cells," *Appl. Phys. Lett.*, vol. 91, no. 26, p. 263505, Dec. 2007.

[53] X. Gu *et al.*, "A solution-processed hole extraction layer made from ultrathin MoS 2 nanosheets for efficient organic solar cells," *Adv. Energy Mater.*, vol. 3, no. 10, pp. 1262–1268, Oct. 2013.

[54] H. Q. Wang, N. Li, N. S. Guldal, and C. J. Brabec, "Nanocrystal V2O5 thin film as hole-extraction layer in normal architecture organic solar cells," *Org. Electron.*, vol. 13, no. 12, pp. 3014–3021, Dec. 2012.

[55] T. Stubhan, N. Li, N. A. Luechinger, S. C. Halim, G. J. Matt, and C. J. Brabec, "High fill factor polymer solar cells incorporating a low temperature solution processed WO3 hole extraction layer," *Adv. Energy Mater.*, vol. 2, no. 12, pp. 1433–1438, Dec. 2012.

[56] W. Chen, F. Z. Liu, X. Y. Feng, A. B. Djurišić, W. K. Chan, and Z. B. He,

"Cesium Doped NiOx as an Efficient Hole Extraction Layer for Inverted Planar Perovskite Solar Cells," *Adv. Energy Mater.*, vol. 7, no. 19, Oct. 2017.

[57] S. Trost, K. Zilberberg, A. Behrendt, and T. Riedl, "Room-temperature solution processed SnO x as an electron extraction layer for inverted organic solar cells with superior thermal stability," *J. Mater. Chem.*, vol. 22, no. 32, pp. 16224–16229, Aug. 2012.

[58] W. Lan *et al.*, "Effect of ZnO Electron Extraction Layer on Charge Recombination and Collection Properties in Organic Solar Cells," *ACS Appl. Energy Mater.*, vol. 2, no. 10, pp. 7385–7392, Oct. 2019.

[59] J. Hu, Y. Shirai, L. Han, and Y. Wakayama, "Template method for fabricating interdigitate p-n heterojunction for organic solar cell," *Nanoscale Res. Lett.*, vol. 7, no. 1, pp. 1–5, Aug. 2012.

[60] D. Bartesaghi *et al.*, "Competition between recombination and extraction of free charges determines the fill factor of organic solar cells," *Nat. Commun.*, vol. 6, no. 1, pp. 1–10, May 2015.

[61] "Fundamentals of Photovoltaics | Mechanical Engineering | MIT OpenCourseWare." [Online]. Available: https://ocw.mit.edu/courses/mechanical-engineering/2-627-fundamentals-of-photovoltaics-fall-2013/. [Accessed: 08-Jul-2020].

[62] L. Tous *et al.*, "Large area copper plated silicon solar cell exceeding 19.5% efficiency," in *Energy Procedia*, 2011, vol. 21, pp. 58–65.

[63] W. J. Potscavage, S. Yoo, and B. Kippelen, "Origin of the open-circuit voltage in multilayer heterojunction organic solar cells," *Appl. Phys. Lett.*, vol. 93, no. 19, p. 193308, Nov. 2008.

[64] H. Hoppe and N. S. Sariciftci, "Organic solar cells: An overview," *J. Mater. Res.*, vol. 19, no. 7, pp. 1924–1945, Jul. 2004.

[65] B. Mazhari, "An improved solar cell circuit model for organic solar cells," *Sol. Energy Mater. Sol. Cells*, vol. 90, no. 7–8, pp. 1021–1033, May 2006.

[66] F. Zhang, O. Inganäs, Y. Zhou, and K. Vandewal, "Development of polymer-fullerene solar cells," *Natl. Sci. Rev.*, vol. 3, pp. 222–239, 2016.

[67] M. C. Scharber and N. S. Sariciftci, "Efficiency of bulk-heterojunction organic solar cells," *Progress in Polymer Science*, vol. 38, no. 12. Pergamon, pp. 1929–1940, 01-Dec-2013.

[68] A. Karki *et al.*, "Understanding the High Performance of over 15% Efficiency in Single-Junction Bulk Heterojunction Organic Solar Cells," *Adv. Mater.*, vol. 31, no. 48, p. 1903868, Nov. 2019.

[69] N. C. Giebink, G. P. Wiederrecht, M. R. Wasielewski, and S. R. Forrest, "Thermodynamic efficiency limit of excitonic solar cells," *Phys. Rev. B - Condens. Matter Mater. Phys.*, vol. 83, no. 19, p. 195326, May 2011.

[70] H. Yu, Y. Ge, and S. Shi, "Improving power conversion efficiency of polymer solar cells by doping copper phthalocyanine," *Electrochim. Acta*, vol. 180, pp. 645–650, Oct. 2015.

[71] T. C. Wu *et al.*, "Singlet fission efficiency in tetracene-based organic solar cells," *Appl. Phys. Lett.*, vol. 104, no. 19, p. 193901, May 2014.

[72] P. M. Zimmerman, F. Bell, D. Casanova, and M. Head-Gordon, "Mechanism for singlet fission in pentacene and tetracene: From single exciton to two triplets," *J. Am. Chem. Soc.*, vol. 133, no. 49, pp. 19944–19952, Dec. 2011.

[73] H. Q. Wang, T. Stubhan, A. Osvet, I. Litzov, and C. J. Brabec, "Up-conversion semiconducting MoO 3:Yb/Er nanocomposites as buffer layer in organic solar cells," *Sol. Energy Mater. Sol. Cells*, vol. 105, pp. 196–201, Oct. 2012.

[74] L. Yang, L. Yan, and W. You, "Organic solar cells beyond one pair of donor-acceptor: Ternary blends and more," *Journal of Physical Chemistry Letters*, vol. 4, no. 11. American Chemical Society, pp. 1802–1810, 2013.

[75] S. Ren *et al.*, "Inorganic-organic hybrid solar cell: Bridging quantum dots to conjugated polymer nanowires," *Nano Lett.*, vol. 11, no. 9, pp. 3998–4002, Sep.

2011.
[76] S. Ren, N. Zhao, S. C. Crawford, M. Tambe, V. Bulović, and S. Gradeĉak, “Heterojunction photovoltaics using GaAs nanowires and conjugated polymers,” *Nano Lett.*, vol. 11, no. 2, pp. 408–413, Feb. 2011.
[77] N. Radychev, I. Lokteva, F. Witt, J. Kolny-Olesiak, H. Borchert, and J. Parisi, “Physical origin of the impact of different nanocrystal surface modifications on the performance of CdSe/P3HT hybrid solar cells,” *J. Phys. Chem. C*, vol. 115, no. 29, pp. 14111–14122, Jul. 2011.
[78] Y. Firdaus *et al.*, “Enhancement of the photovoltaic performance in P3HT: PbS hybrid solar cells using small size PbS quantum dots,” *J. Appl. Phys.*, vol. 116, no. 9, p. 094305, Sep. 2014.
[79] L. He, C. Jiang, Rusli, D. Lai, and H. Wang, “Highly efficient Si-nanorods/organic hybrid core-sheath heterojunction solar cells,” *Appl. Phys. Lett.*, vol. 99, no. 2, p. 021104, Jul. 2011.
[80] S. Avasthi, S. Lee, Y. L. Loo, and J. C. Sturm, “Role of majority and minority carrier barriers silicon/organic hybrid heterojunction solar cells,” *Adv. Mater.*, vol. 23, no. 48, pp. 5762–5766, Dec. 2011.
[81] X. Shen, B. Sun, D. Liu, and S. T. Lee, “Hybrid heterojunction solar cell based on organic-inorganic silicon nanowire array architecture,” *J. Am. Chem. Soc.*, vol. 133, no. 48, pp. 19408–19415, Dec. 2011.
[82] L. He, Rusli, C. Jiang, H. Wang, and D. Lai, “Simple approach of fabricating high efficiency Si nanowire/conductive polymer hybrid solar cells,” *IEEE Electron Device Lett.*, vol. 32, no. 10, pp. 1406–1408, Oct. 2011.
[83] L. He, C. Jiang, H. Wang, D. Lai, and Rusli, “High efficiency planar Si/organic heterojunction hybrid solar cells,” *Appl. Phys. Lett.*, vol. 100, no. 7, p. 073503, Feb. 2012.
[84] A. Anctil, C. Babbitt, B. Landi, and R. P. Raffaelle, “Life-cycle assessment of organic solar cell technologies,” in *Conference Record of the IEEE Photovoltaic Specialists Conference*, 2010, pp. 742–747.
[85] D. J. Burke and D. J. Lipomi, “Green chemistry for organic solar cells,” *Energy and Environmental Science*, vol. 6, no. 7. Royal Society of Chemistry, pp. 2053–2066, 19-Jul-2013.
[86] Y. Zhou *et al.*, “Recyclable organic solar cells on cellulose nanocrystal substrates,” *Sci. Rep.*, vol. 3, no. 1, pp. 1–5, Mar. 2013.
[87] C. J. Brabec, J. A. Hauch, P. Schilinsky, and C. Waldauf, “Production aspects of organic photovoltaics and their impact on the commercialization of devices,” *MRS Bulletin*, vol. 30, no. 1. Materials Research Society, pp. 50–52, 2005.
[88] B. Conings *et al.*, “Modeling the temperature induced degradation kinetics of the short circuit current in organic bulk heterojunction solar cells,” *Appl. Phys. Lett.*, vol. 96, no. 16, p. 163301, Apr. 2010.
[89] K. Kawano, R. Pacios, D. Poplavskyy, J. Nelson, D. D. C. Bradley, and J. R. Durrant, “Degradation of organic solar cells due to air exposure,” *Sol. Energy Mater. Sol. Cells*, vol. 90, no. 20, pp. 3520–3530, Dec. 2006.
[90] J. Adams *et al.*, “Water Ingress in Encapsulated Inverted Organic Solar Cells: Correlating Infrared Imaging and Photovoltaic Performance,” *Adv. Energy Mater.*, vol. 5, no. 20, p. 1501065, Oct. 2015.
[91] M. Jørgensen, K. Norrman, and F. C. Krebs, “Stability/degradation of polymer solar cells,” *Solar Energy Materials and Solar Cells*, vol. 92, no. 7. North-Holland, pp. 686–714, 01-Jul-2008.